

APPENDIX C: SENSITIVITY ANALYSIS OF MULTI-SCALE SIR MODEL WITH EXPONENTIALLY DISTRIBUTED INFECTIOUS PERIOD

Methods

To investigate how the spatial configuration of counties and spatial heterogeneities influence long-term epidemic dynamics, we compared our multi-scale SIR model with exponentially distributed extirpation time simulation results initialized in Schoharie County with 250 simulations initialized in the northwest (Clackamas County, Oregon), southwest (Pima County, Arizona), southeast (Gadsden County, Florida) and in the interior highlands (Marion County, Arkansas). Counties from the northwest, southwest and southeast regions were chosen to represent geographically distinct nodes that are distant from Schoharie County in the landscape graph. Marion County in Arkansas was selected because it is located in a region of high cave density (Fig. A3). To ascertain which counties are at the greatest risk of infection and if disease risk is greater close to the epidemic epicenter, we generated heat maps indicating the fraction of simulations for which each county was infected (Figs. C1–C4). To investigate how location of the introduction and spatial configuration of the landscape impact long-term epidemic dynamics and to clarify the factors that determine the final size of the epidemic, we generated the epidemic final size distribution, incidence and prevalence statistics from these simulations (Figs. C6–C8). To determine the sensitivity of our results to county-level heterogeneities, we executed 1,000 simulations of the epidemic starting from Schoharie County assuming time to epidemic burnout was ten years for all counties (the median county-level epidemic duration). This ensured that all infected nodes were eliminated from the graph ten years following year of infection (Fig. C5). To investigate the influence of climate heterogeneities on long-term epidemic dynamics, we initialized 250 simulations from Clackamas County, Oregon, assuming an homogeneous winter duration, equal to the longest winter, in all counties (Fig. C9).

Results

We assessed the influence of different spatial initial conditions on spatiotemporal spread of the infection. Figs. C1–C3 show that geographic regions with large numbers of hibernacula and highly connected habitat, such as the northeast and Ozarks, have the greatest risk of infection. This result indicates that the long-term infection risk of these key regions is insensitive to the location of the county in which the infection may be first detected. However, infections initialized in Gadsden County, Florida, fail to take off (Fig. C4). The climate in this region leads to stochastic fadeout of the infection before establishment. It is also interesting to note that in contrast to infections introduced to Schoharie County and Marion County in Arkansas (Figs. B2 and C1 respectively), which are located within highly connected landscape, most counties close to the site of introduction in Figs. C2 and C3 do not have a near-certain probability of infection. This suggests that the high final epidemic sizes for the regional bat population in the northeast calculated in Fig. 3 in the main text are not resulting from proximity to the origin of the introduction, but are due to the features of the northeastern landscape, which provide the ideal conditions for rapid propagation of WNS. These results support the hypothesis that geographic corridors facilitate the spread of WNS (Maher et al. 2012).

Theory predicts bimodality of the epidemic final size distribution, i.e., there is a non-zero probability of stochastic fadeout before the epidemic takes off (Daley and Gani, 2001). Fig. C6 shows the epidemic final size distributions computed from simulations initialized in the interior highlands (A), southeast (B), northwest (C), southwest (D) and Schoharie County (E). Not surprisingly, the macro-scale epidemic failed to take off from a single introduction in Florida, a sub-tropical region with a short winter, in 87% of simulations (Fig. C6(B)). For the epidemics that did take off, the median final size was 85%. While the location of the epidemic origin did not affect median final size (at ~85% for all epicenters except Florida), it did impact the shape of the final size distribution. A single introduction to the northwest and southwest both led to a non-zero probability of no epidemic (bimodal final size distribution with 4% and 14% of simulations with no epidemic respectively (Figs. C6(C) and C6(D))). By contrast, the

final size distribution of epidemics originating from the interior highlands was unimodal about the mean, similar to that from Schoharie County (Figs. C6(A) and C6(E)). We additionally note that the final size distribution of epidemics with Schoharie County as the epicenter only becomes bimodal for extremely short hibernaculum extirpation times (approximately less than 100 days), suggesting that there is a very low probability of stochastic fadeout for infections introduced to the main geographic corridor.

To investigate how location of the introduction and spatial configuration of the landscape impact epidemic dynamics, we generated macro-scale incidence (number of newly infected counties) and prevalence (proportion of infected counties) statistics (Figs. C7–C9). In contrast to epidemics beginning in Schoharie County, the propagation of the infection was much slower and subject to greater stochastic variability in simulations initialized in the northwest and southwest, with prevalence and incidence not peaking until the 2020s and 2030s respectively (Figs. C7 and C8, (C) and (D)). However, median incidence and prevalence calculated from epidemics initialized from the interior highlands closely resembled those initialized from Schoharie County. From this analysis we conclude that epidemic take off is more likely to be slower and subject to greater stochasticity in regions that are warmer and are isolated from the main mountainous regions of the West, the Appalachians and the Ozarks, where hibernacula are plentiful (Culver et al. 1999, Humphrey 1975). Moreover, there is a non-zero probability of no epidemic in these isolated regions.

We also determined the impact of landscape heterogeneities on epidemic dynamics by considering homogeneity of nodes in epidemic and winter durations (i.e., the largest mean number of days below 10 °C) separately. Assuming homogeneous county-scale epidemics with durations equal to the median duration of ten years, we found that the final size distribution was unimodal with a mean of 77% (Fig C6(F)), slightly less than that predicted by the multi-scale SIR model, and median prevalence dropped off sharply (Fig C7(D)). Fig. C5 indicates that the probability of spread to the western seaboard is only slightly reduced, with the key regions of the Appalachians, interior highlands and West predicted to be infected with very high probability. However, spread under this model to western and southern Texas, a region with a large number of potential hibernacula, was found to be less likely, suggesting that

the large numbers of potential hibernacula will facilitate spread in that region. In addition, we investigated if long winters in every county would lead to faster spread in the initial stages of the epidemic from a more isolated region. Simulating epidemics from Clackamas County, Oregon, leads to a final mean epidemic size of ~99%, and the probability that the epidemic does not take off is near zero. However, county homogeneity in winters of long duration does not remove the stochastic variability in the initial propagation of the infection (cf. Figs. C9(A) and C7(C), Figs. C9(B) and C8(C)). Take off is still slow, and propagation of the infection is likely to be via long-distance jump dispersal. However, once the infection reaches the main cave-bearing corridors, spread of WNS is rapid, and is accelerated by the homogeneity in winters of long duration. We conclude that long winters alone will not lead to explosive spread of the infection but temperature gradients and geographic corridors together facilitate rapid expansion of the disease. These results suggest that county heterogeneities are likely to contribute to both the initial propagation of the epidemic and the final size of the macro-scale epidemic.

SUPPORTING FIGURES FOR SENSITIVITY ANALYSIS

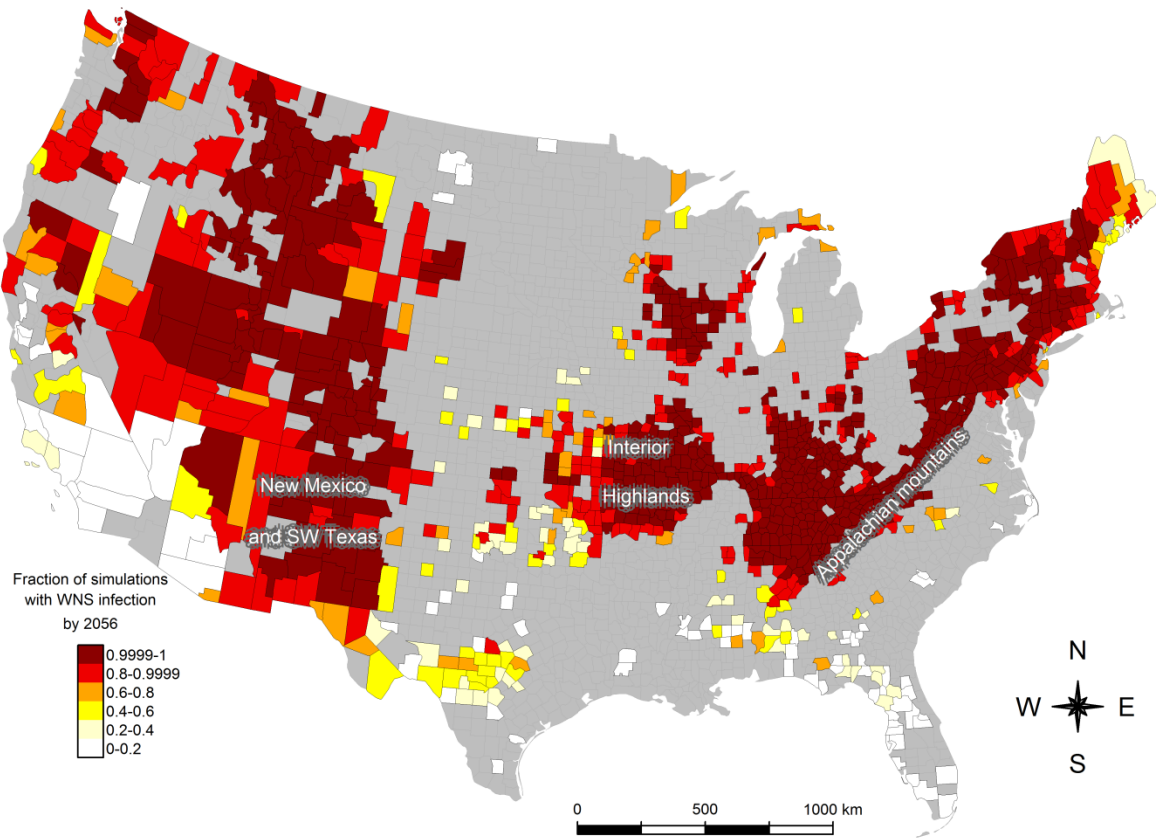


FIG. C1. The spread of White-nose Syndrome in the contiguous United States, given a single introduction to the interior highlands. Counties are colored according to the fraction of simulations that they were infected with WNS out of 250 simulations. All simulations were initialized using a single infected county (Marion County, Arkansas) in the interior highlands. Counties colored grey have no caves and were excluded from the model. The pattern of infection is similar to Fig. B2.

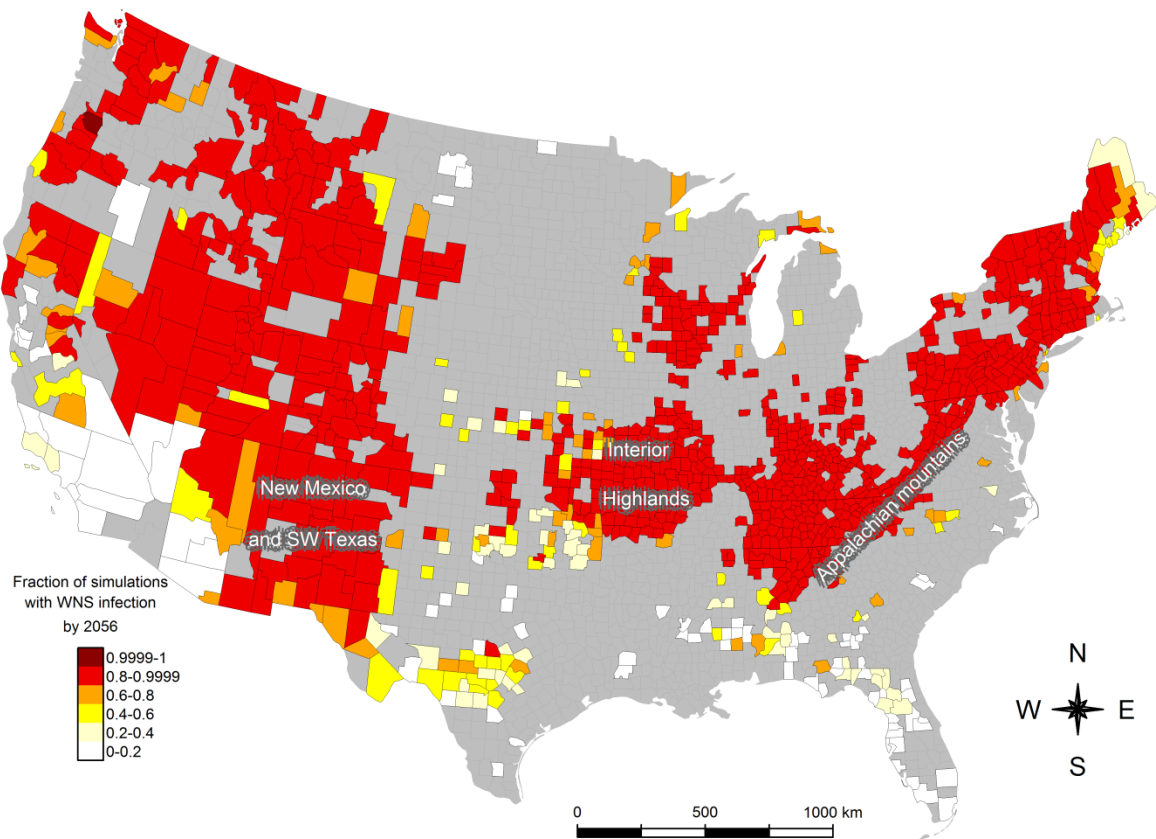


FIG. C2. The spread of White-nose Syndrome in the contiguous United States, given a single introduction to the northwest. Counties are colored according to the fraction of simulations that they were infected with WNS out of 250 simulations. All simulations were initialized using a single infected county (Clackamas County, Oregon) in the northwest. Counties colored gray have no caves and were excluded. The pattern of infection is similar to Fig. B2. Close to the origin the probability of infection is higher than in Fig. B2 but the probability of spread to the northeast is still very high.

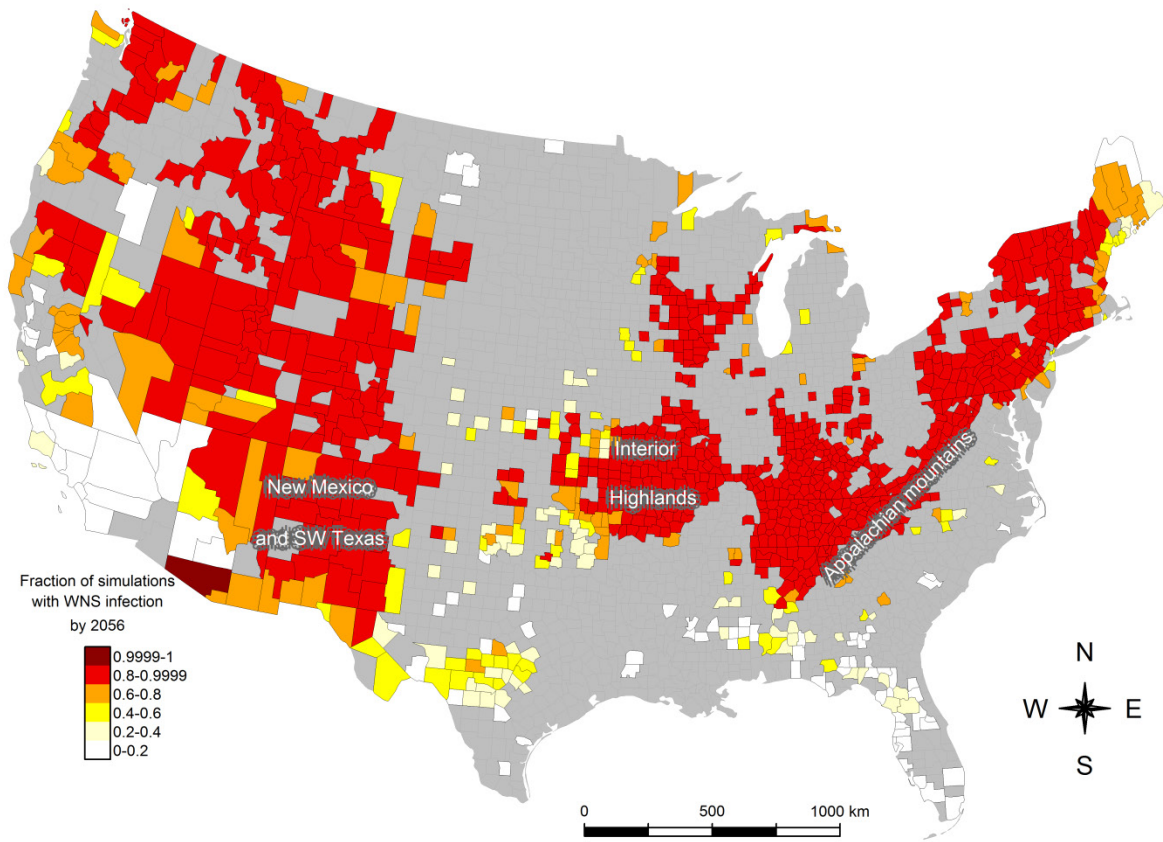


FIG. C3. The spread of White-nose Syndrome in the contiguous United States, given a single introduction to the southwest. Counties are colored according to the fraction of simulations that they were infected with WNS out of 250 simulations. All simulations were initialized using a single infected county (Pima County, Arizona) in the southwest. Counties colored grey have no caves and were excluded from the model. The pattern of infection is similar to Fig. B2. Close to the origin the probability of infection is higher than in Fig. B2 but the probability of spread to the northeast is still very high.

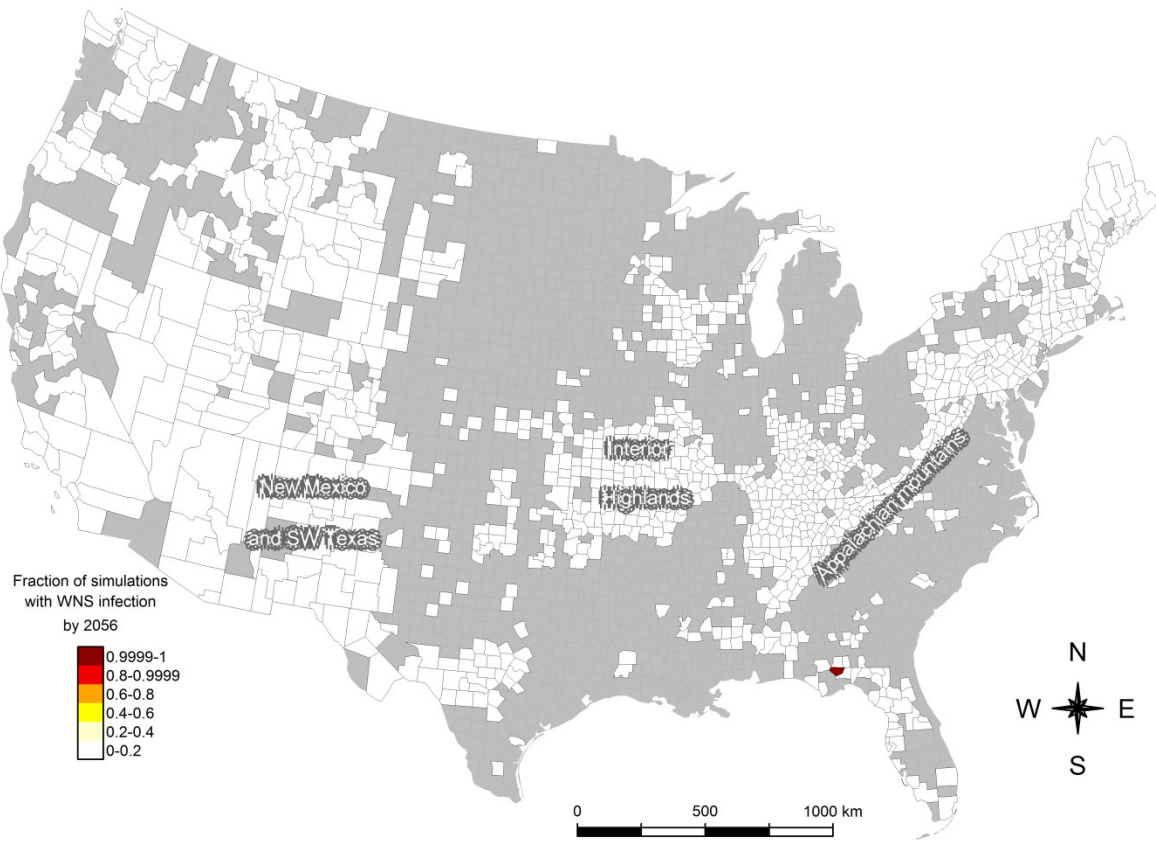


FIG. C4. The spread of White-nose Syndrome in the contiguous United States, given a single introduction to the southeast. Counties are colored according to the fraction of simulations that they were infected with WNS out of 250 simulations. All simulations were initialized using a single infected county (Gadsden County, Florida) in the southeast. Counties colored grey have no caves and were excluded from the model.

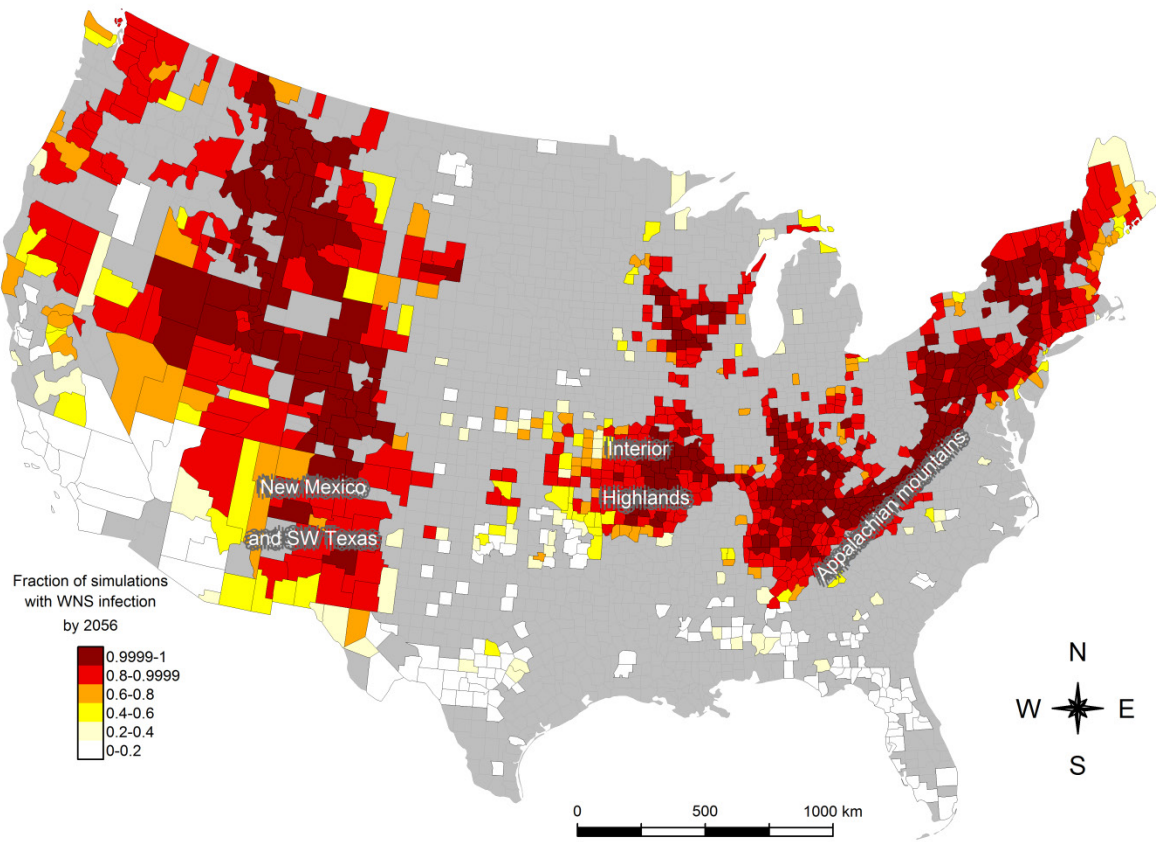


FIG. C5. The spread of White-nose Syndrome in the contiguous United States, given a homogeneous epidemic duration of 10 years in each county. Counties are colored according to the fraction of simulations that they were infected with WNS out of 1,000 simulations. All simulations were initialized with Schoharie County, New York. Counties colored gray have no caves and were excluded from the model. The pattern of infection is fairly similar to Fig. B2 but regions of the southeast and Texas are less likely to be infected.

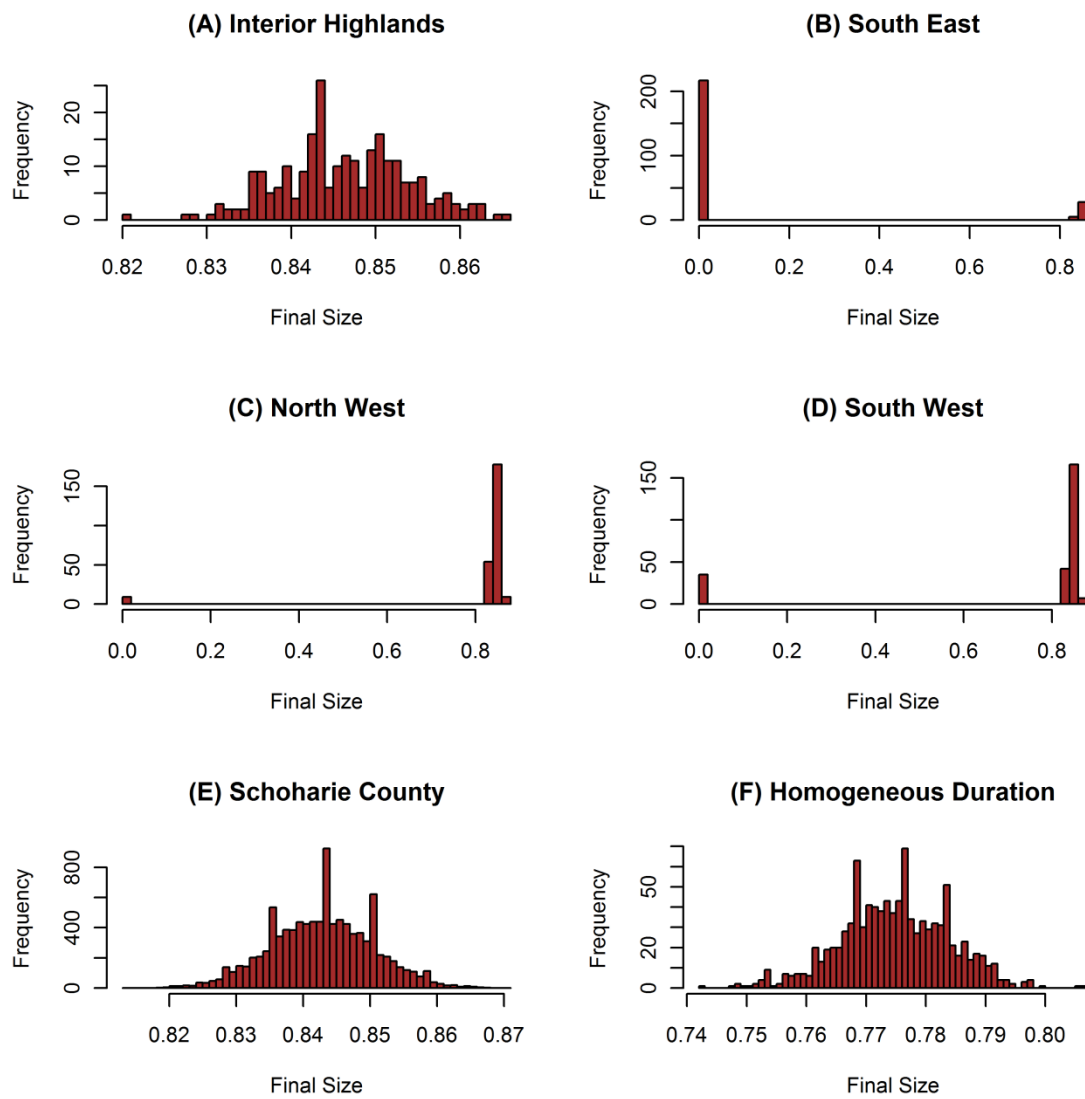


FIG. C6. Macro-scale final size distributions. (A) (B) (C) and (D) The final size distribution for 250 simulations that begin in the interior highlands, southeast, southwest and northwest respectively. There is a non-zero probability that no macro-scale epidemic will occur in (B), (C) and (D). (E) The macro-scale final size distribution for 10,000 simulations that begin in Schoharie County (the mean of this distribution is marked by the cross in Fig. 3 of the main text). (F) The macro-scale final size distribution for 1,000 simulations that begin in Schoharie County but assume equal durations of the epidemic in each node. Final sizes in this case are lower than those in (E).

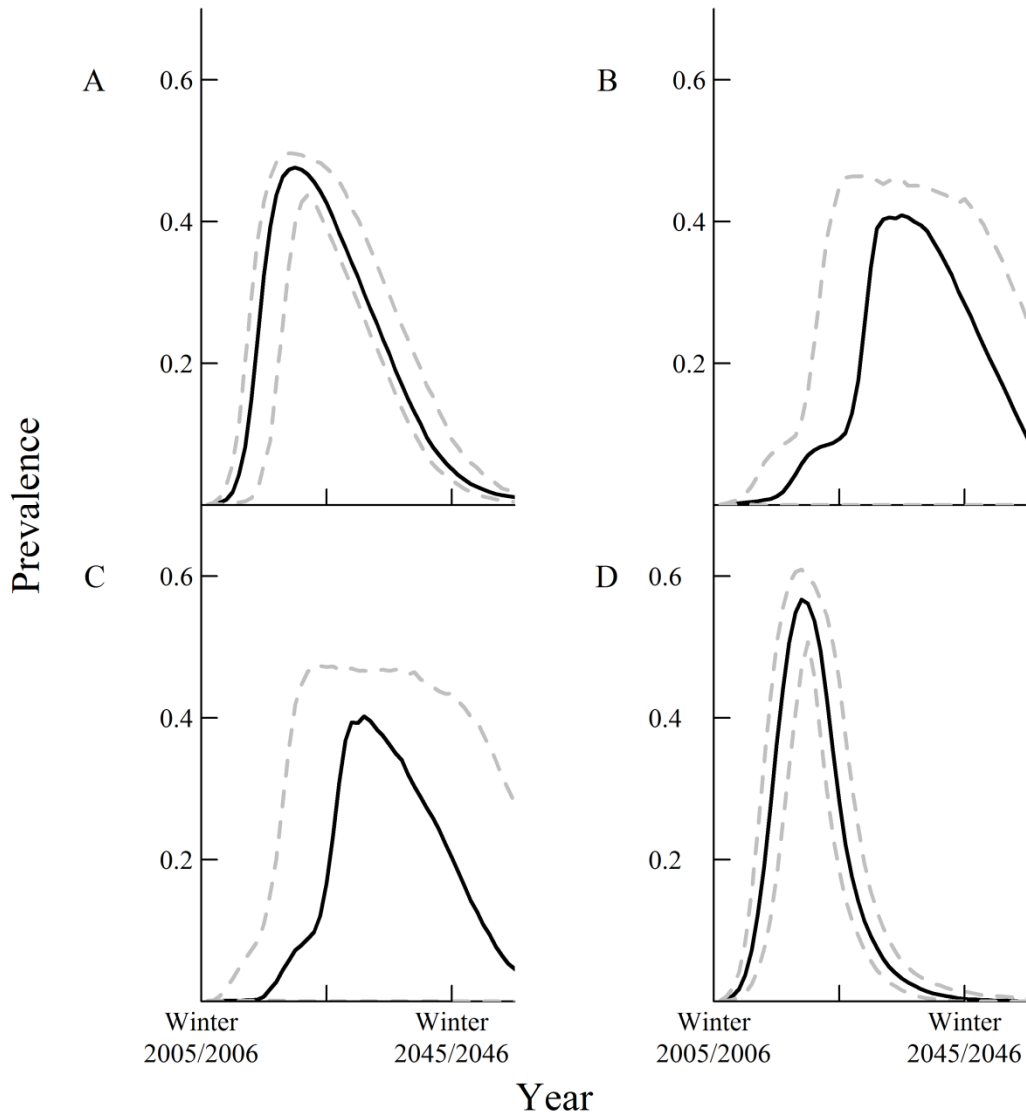


FIG. C7. Macro-scale prevalence of infection following introduction of WNS to different locations. Solid lines are median values and dashed lines represent 95% prediction intervals. (A) Prevalence of infection following introduction of WNS to the interior highlands closely resembles prevalence statistic from Schoharie County in Fig. 2b of the main text. (B) Prevalence following introduction of WNS to the northwest slowly increases, peaking in the winter of 2034–2035. (C) Prevalence following introduction of WNS to the south west slowly increases, peaking in 2030–2031. Prevalence in (A), (B) and (C) declines at approximately the same rate. (D) Prevalence assuming homogeneous epidemic durations peaks in 2018–2019 but falls off much more rapidly than Fig 2b of the main text.

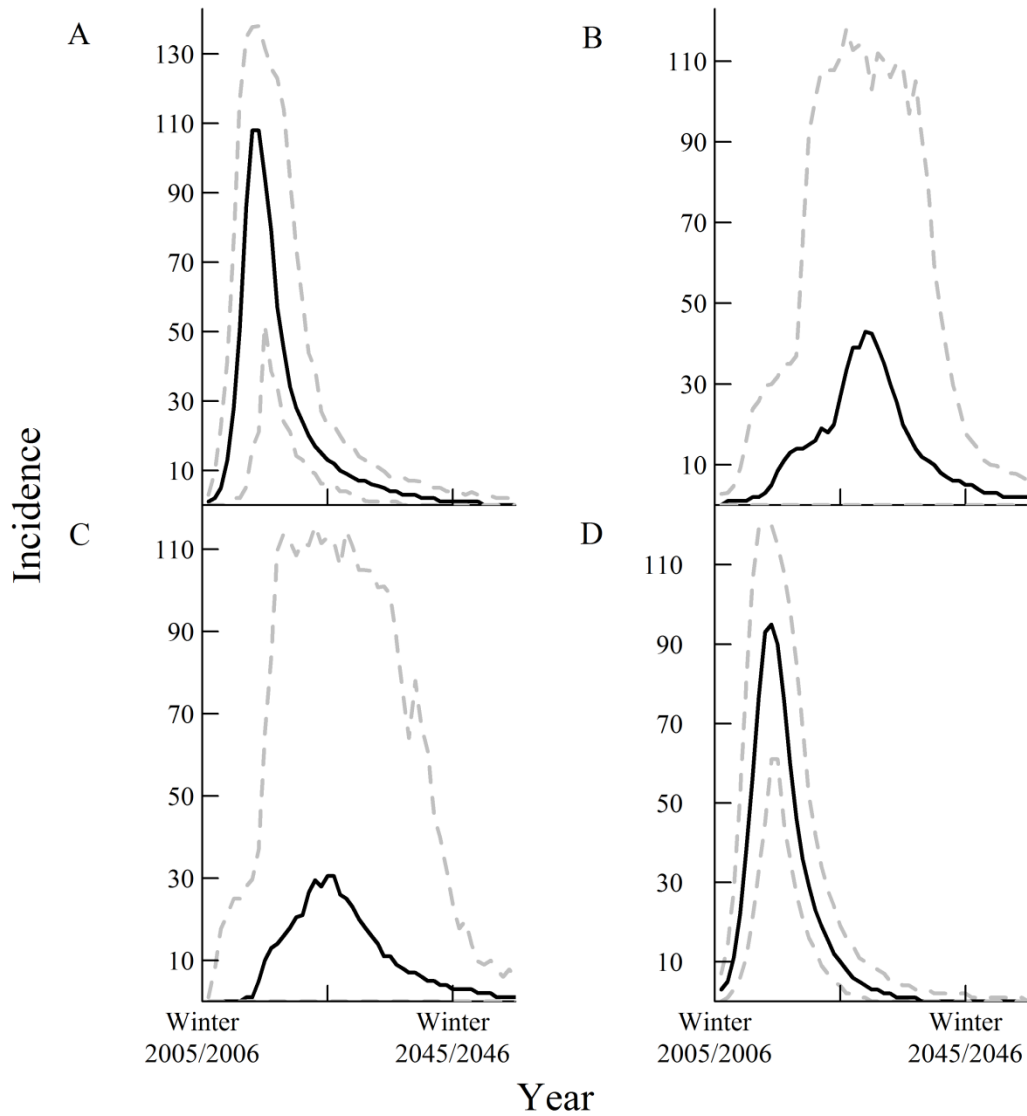


FIG. C8. Macro-scale incidence of infection following introduction of WNS to different locations. Solid lines are median values and dashed lines represent 95% prediction intervals. (A) Incidence of infection following introduction of WNS to the interior highlands closely resembles incidence statistic from Schoharie County in Fig. 2a of the main text, with peak occurring in the winter of 2013–2014. (B) Incidence following introduction of WNS to the northwest slowly increases, peaking in the winter of 2028–2029. (C) Incidence following introduction of WNS to the south west slowly increases, peaking in 2025–2026. (D) Incidence assuming homogeneous epidemic durations peaks in 2013–2014.

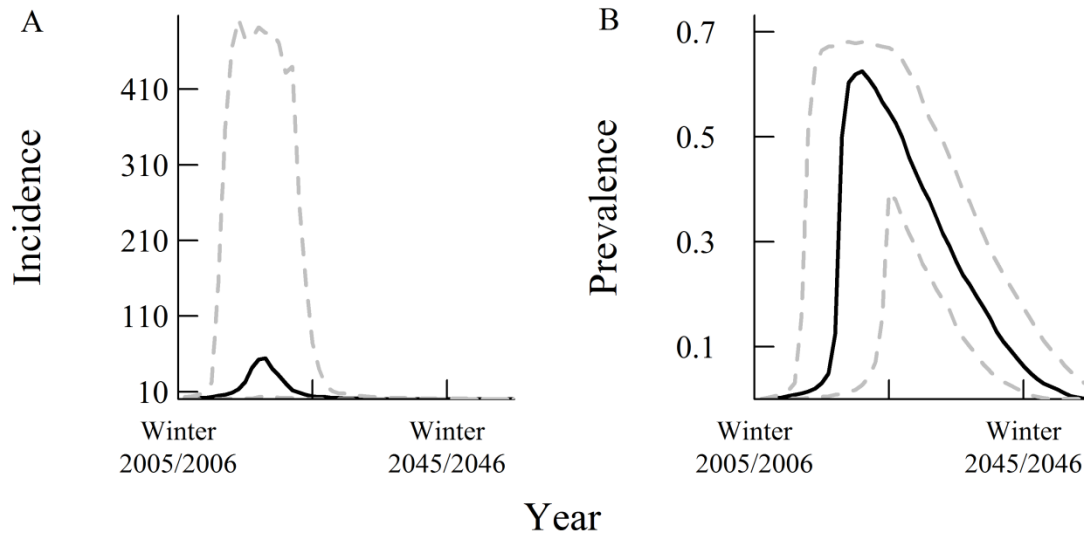


FIG. C9. Macro-scale incidence and prevalence of the infection assuming homogeneous winter duration and introduction of the infection to Clackamas County, Oregon. Solid lines are median values and dashed lines represent 95% prediction intervals. (A) Incidence of the infection is highly stochastic, due to jump dispersal of the infection. (B) Peak prevalence of the infection is very high, as a result of the long winters in each county.

LITERATURE CITED

Culver, D. C., H. H. H. Iii, and M. C. Christman. 1999. Distribution Map of Caves and Cave Animals in the United States. *J Cave Karst Studies* 61:139–140.

Daley, D. J., and J. M. Gani. 2001. *Epidemic Modelling: An Introduction*. Cambridge University Press.

Humphrey, S. R. 1975. Nursery Roosts and Community Diversity of Nearctic Bats. *Journal of Mammalogy* 56(2):321–346. doi:10.2307/1379364

Maher, S. P., A. M. Kramer, J. T. Pulliam, M. A. Zokan, S. E. Bowden, H. D. Barton, and J. M. Drake. 2012. Spread of white-nose syndrome on a network regulated by geography and climate. *Nature Communications* 3:1306. doi:10.1038/ncomms2301